ISSN 0351–2657
HOBUD7 24(1) 1 (2003)

OBSERVATIONAL EVIDENCE FOR A SHOCK EVENT IN THE SOLAR GRANULATION

A. KUČERA[1], J. RYBÁK[1], A. HANSLMEIER[2], H. WÖHL[3]
[1]*Astronomical Institute of the Slovak Academy of Sciences, SK-05960 Tatranská Lomnica, Slovakia*
[2]*Institut für Geophysik, Astrophysik und Meteorologie, Univeritätsplatz 5, A-8010 Graz, Austria*
[3]*Kiepenheuer-Institut für Sonnenphysik, Schöneckstraße 6, D-79104 Freiburg, Germany*

UDC 523.985.3-355
Original scientific paper
(Received September 30, 2000; accepted October 30, 2000)

Abstract. High resolution spectra of Fe II 6456.39 Å line are used to investigate a shock in the solar granulation. The changes of the main spectral characteristics measured in the shock area are in a good agreement with the characteristics predicted with theory. The analysis of the shock, made in the past by several authors was extended in this work to the analysis of a temporal development of the shock event. The 2 minutes duration of a stable and declining phases of the event was studied. We conclude that the observed shock belonged to the particular type of shock generated as a consequence of the swaying motion of the magnetic flux tube concentrated in the intergranular lane. Such type of shock was proposed by numerical simulations made by Steiner et al. 1998.

Key words: Sun - granulation - shocks

1. Introduction

Numerical simulations of the solar granulation made in the last two decades have allowed to study the non-stationary nature of the photospheric layers. First, the solar granulation was simulated as a non-magnetic medium (see for example: Nordlund, 1984, Stein and Nordlund, 1989, Steffen, Ludwig, and Krüss, 1989) Later an assumption of low-viscosity plasma was introduced into the calculations (e.g.,

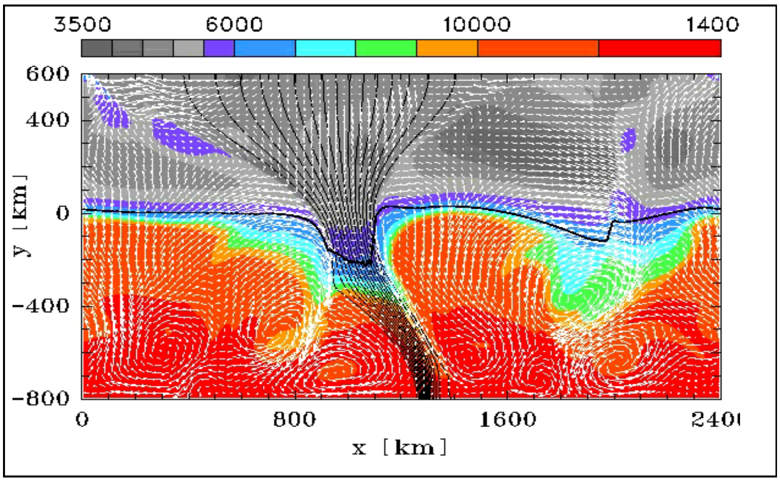

Figure 1: *Two dimensional time dependent numerical simulation of a granulation. The grey-scale (on top) represents temperature in K. The small white arrows show the velocity pattern of the plasma. Magnetic field lines are represented by a bundle of nearly vertical lines. (According Steiner et al. 1998)*

Cattaneo et al., 1989, Malagoli et al., 1990, Steffen & Freytag, 1991, Gadun et al., 1999). After several attempts to deal also with an influence of magnetic field on the granular convection (e.g., Deinzer et al., 1984, Knölker et al., 1988, Grossman-Doerth et al., 1988) fully appropriate treatment of the non-stationary nature of the solar photosphere harboring also the magnetic field and the low viscosity plasma was done by Steiner et al. 1998. Fig. 1 shows one snapshot of time series of such calculations. Introducing the magnetic field (2D simulations) led to detection of three types of shocks in the solar granulation

The *type-a* shock belongs to the deceleration zone of the horizontal granular flow just on the edge of the intergranular lane (see Fig. 2). This type is in agreement with the previously predicted shock from non-magnetic simulations made by Cattaneo et al. (1989, 1990) and other authors.

The *type-b* shock is caused by a swaying motion of the flux tube which pushes the plasma fast in front of it creating a shock moving horizontally and oriented vertically.

The *type-c* shock was found to be propagated upward within the flux sheet. This type is generated by the instability of the flux tube caused by convection.

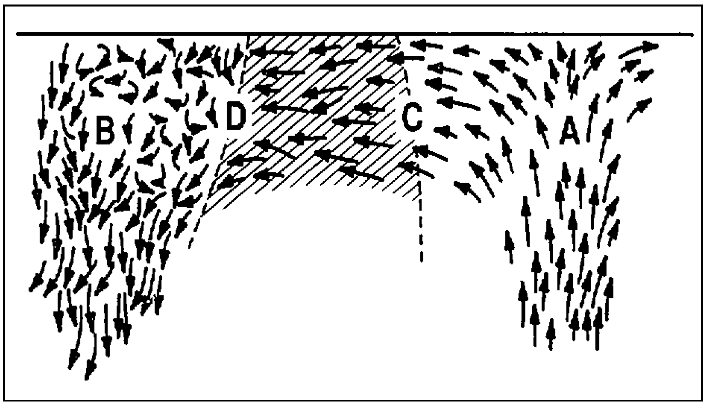

Figure 2: *Schematic sketch of the type-a shock in the intergranular lane taken from the work of Nesis et al. (1992). The plasma flows from granule (A) to intergranular space (B). The velocity of the plasma reaches and exceeds the sound speed in the space between (C) and (D). The shock is generated in the space between (D) and (B) and turbulence increases in that place as a consequence of the shock.*

When the radiation transfer codes were included to the simulations it was possible to extend the work up to the predictions of the spectral profiles of the lines originated in the modeled solar photosphere. Thus a possibility for direct comparison of the spectra observed with high spatial and spectral resolution in the solar granulation and line profiles predicted by the numerical simulations arisen. The first attempt to confirm existence of supersonic horizontal flows (*type-a* shock) was made by Nesis et al. (1992). High resolution observations made by Solanki et al., (1996) confirmed qualitatively the trend of relation found by Nesis et al. (1992).

The aim of this paper is to extend the direct evidence of the shocks in low solar photosphere to direct evidence of temporal development of such event. We used (as recommended by Gadun et al. 1999) high spatial and spectral resolution observations of Fe II spectral line 6456.39 Å near the solar limb.

2. Observations

After careful selection of the Fe II lines in the visible range of spectrum the Fe II line 6456.39 Å was selected when the limitation given by the spectrograph were considered. The main characteristics of the line are given in Table 1. Observa-

λ^1[Å]	Multip.[2]	$E_p{}^3$[eV]	Transit.[4]	$W_\lambda{}^5$[mÅ]	L. fact.[4]
6456.388	74	3.903	$b^4D_{3\frac{1}{2}}$-$z^4P_{2\frac{1}{2}}$	81	1.214/1.182

Table 1: The atomic parameters of Fe II line selected for observations. The E_p and W_λ mean the excitation potential of the lower level and the equivalent width of the line respectively. The Landé factors are given for the cases of LS coupling and the empirical values. (References : 1 – Allende Prieto and Garciá López, 1998, 2 – Moore, 1972, 3 – Kurucz, 1990, 4 – Solanki and Stenflo, 1985, 5 – Moore et al., 1966).

tions were carried out on April 27, 2000 with the Vacuum Tower Telescope (VTT) with large Echelle spectrograph (Schröter et al. 1985) at Observatorio del Teide, Tenerife, Spain. The adaptive optics (AO) developed at the National Solar Observatory, Sacramento Peak, Sunspot, USA[1] was used to compensate for pointing errors caused by guiding inaccuracies and seeing. The slit-jaw image i.e. the position of the spectrograph slit on the projected solar surface was recorded with G-band filter of 9 Å bandpass centered at 4306 Å. The spectrograph slit of the width of 100 μm (equivalent to 0.5") was oriented perpendicularly to the horizon to allow the compensation for the differential refraction.

The spectral data were taken with 12 bit XEDAR CCD camera providing 1k$\times$1k spectral images with spatial resolution of 0.125"/pixel. The spectral resolution was 3.09 mÅ/pixel. The exposure time was 1 second and the temporal resolution of the time series was 3 seconds. The DALSA digital camera operated with an exposure time of 5 millisecond and with a cadence of 2 frames per second was used for the SJ system. The whole observing run started at 10:20:54 UT and lasted 15 minutes.

The target near the solar limb (μ=0.648) in the active region NOAA 8967 was selected for observations and the small spot in the region served as a target for AO tracking.

3. Data Reduction

The spectra were photometrically reduced using the precise reduction procedure to eliminate the temporal changes of the flat field conditions (Wöhl et al., 2002). The zero point of the wavelength scale was adjusted according to the average positions of lines derived from all spectra of the run. The polynomial approximation of

[1] http://www.sunspot.noao.edu/AOWEB/

the dispersion was determined from the averaged spectrum taken at disk center using the standard wavelengths from work of Moore et al. (1966). The reference continuum intensity was calculated as the average value of the continua of all spectra of the run. The SJ images acquired during the best seeing conditions were selected for co-alignement with the spectra.

The spectral characteristics: *ic* - the continuum intensity, *ir* - the residual line intensity, *vd* - the Doppler velocity of the line, *fw* - the full width at half depth and *ew* - the equivalent width of the line were calculated for each spectral line in all spectra of the run. The Doppler velocities *vd*, were adjusted to the mean position of the line. The far wings of the line were excluded when the equivalent widths have been calculated to prevent contamination by blended lines.

4. Spectral characteristic of the shock event

The numerical simulations which included the radiative transfer calculation predicted that significant changes of the spectral characteristics should appear in the spectra taken in the shock area in the photosphere. But due to smearing effects caused by the seeing and imperfections of the instrument, only high spatial resolution spectra cloud be used for detection of the changes.

One of the most evident signature of the shock is the significant increase of the full width at half depth *fw*. The increase goes up to 100% when smearing of 0.5" spatial resolution is applied to simulate real observations. Big advantage of the observations made near the limb is that one can rule out the possibility that the same effect of the increase of the *fw* can be caused by the downward motion in the intergranular space.

The second shock signature is an increase of the residual line intensity *ir* as the shock heats the surrounding plasma. The increase of the *ir* caused by the shock was found to be 75% compared to the unaffected value when the artificial degradation for the expected seeing and instrumental effects are included in calculations.

Simulations have outlined also a radical jump of the Doppler velocity *vd*. Jumps greater than 5 km/s marked the change of the direction of the velocity of the plasma in the shock. The observed value of the velocity jump should be expected much smaller due to the smearing by seeing effects and the relative projection of the shock to the line-of-sight. The velocity jump pronounced as a line shift is undetectable with low spatial resolution or when the shock is oblique relatively to the line-of-sight.

Only very small or none change of the continuum intensity *ic* caused by the shocks was reported. Also small changes of the equivalent width of the lines *ew* appear in shocks because an increase of the *fw* is roughly compensated by a decrease of the residual intensity *ir*.

Generally, observations along the longest dimension of the shock strongly enhances chance to register the shock in the spectral profile. Therefore the targets selected near the limb would increase the chance to detect the shock.

5. Results

The quite part of the photosphere in the data set was used to trace the shock in the spectral characteristics. Due to the highest chance to notice the shock in the full width at half depth of line *fw* we concentrated our effort to this characteristic.

Twelve events in total which had the *fw* larger then 10 % compared to the mean value were found in the set. Temporal durations of the events were between 1 - 3 minutes. The most significant event positioned at μ=0.646 was selected for further analysis. The spectral characteristics of *ir*, *vd* and *fw* are shown in Fig. 3 and the less sensitive spectral characteristics *ic* and *ew* are given in Fig. 4. The 'rms' of the *ic* is added in Fig. 4 to demonstrate the changes of the seeing conditions during the observation of the event. Only stationary and decaying phase of the shock can be followed in the Figs. 3 and 4 because the onset of the event had began before the start of our observation. To display clearly the characteristics of the shock, there are shown in Fig. 5 the representative spatial scans of the spectral characteristics extracted from Figs. 3 and 4 for three moments of the development of the shock and for one reference moment taken after the shock. Comparison of the characteristics displayed in Figs 3, 4 and 5 serves for the extracting of the following relations:
The shock is confined to a spatial extent of 0.5 arcsecond and it does not change its position during the event. The maximum value of *fw* is 97 mÅ so it is of 30 % more then the corresponding average value. The stationary phase of the event had a duration of about 1.3 min. Then the decline phase which lasted 0.7 min started.

The maximum values of the line center intensity *ir* are co-spatial with the maximum values of the *fw*. The *ir* values up to 0.61 % of *ic* were measured. It corresponds to a relative change of 11 % of the *ir* when compared to the average value. The enhancement of the continuum intensity *ic* is located in granular structure so it is good marked that the enhancement of the *fw* is located directly on the edge of the granule where the gradient of the *ic* is maximal.

The maximum of the *fw* is not co-spatial with the extreme Doppler velocity values *vd* but it is co-spatial with the gradient of the Doppler velocity *vd*. The gradient is greater than 150 m/s across 0.1 arcsecond. The difference of the total Doppler velocity of the event was found to be up to 1200 m/s just across 1 arcsecond. The velocity of 300 m/s toward the observer was detected at the exact position of the event. A significant velocity difference was found during the evolution of the shock when the change for more than 1000 m/s was detected. No correction for the 5 min velocity oscillations has been performed. Nevertheless the relative small-scale variations of Doppler velocity on the scale of an 1 arcsecond are real.

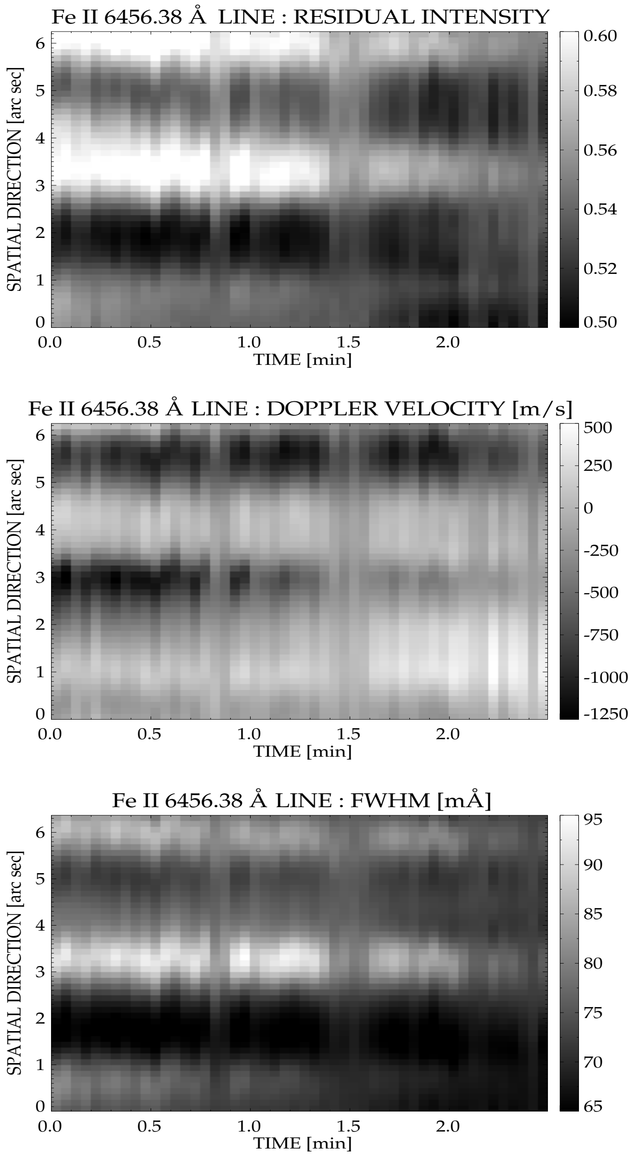

Figure 3: 2D maps (time-space) of the spectral characteristics of *ir*, *vd* and *fw* of the Fe II 6456.39 Å line around the selected granular shock event. The shock event is located at spatial position 3.3" and its duration (∼2 minutes) is clearly seen in the *fw* characteristic.

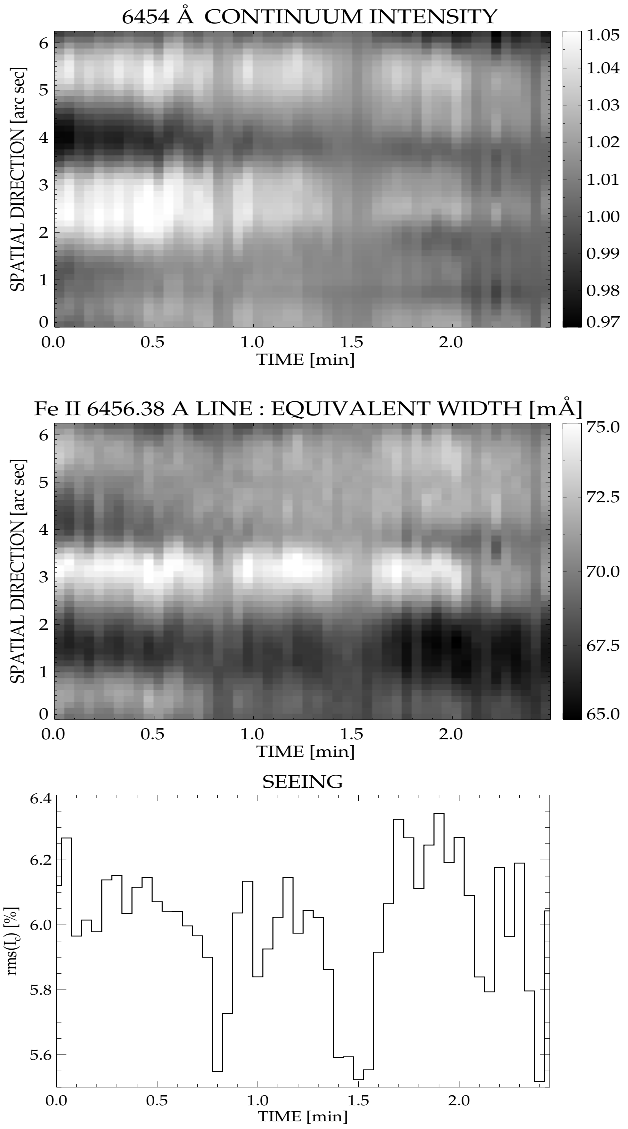

Figure 4: 2D maps (time-space) of the spectral characteristics of *ic* and *ew* of the Fe II 6456.39 Å line around the selected granular shock event. The shock event is located at spatial position 3.3" and its duration was ∼2 minutes. The 'rms' of the *ic* (seeing) show the changes of the seeing conditions during the observation of the event.

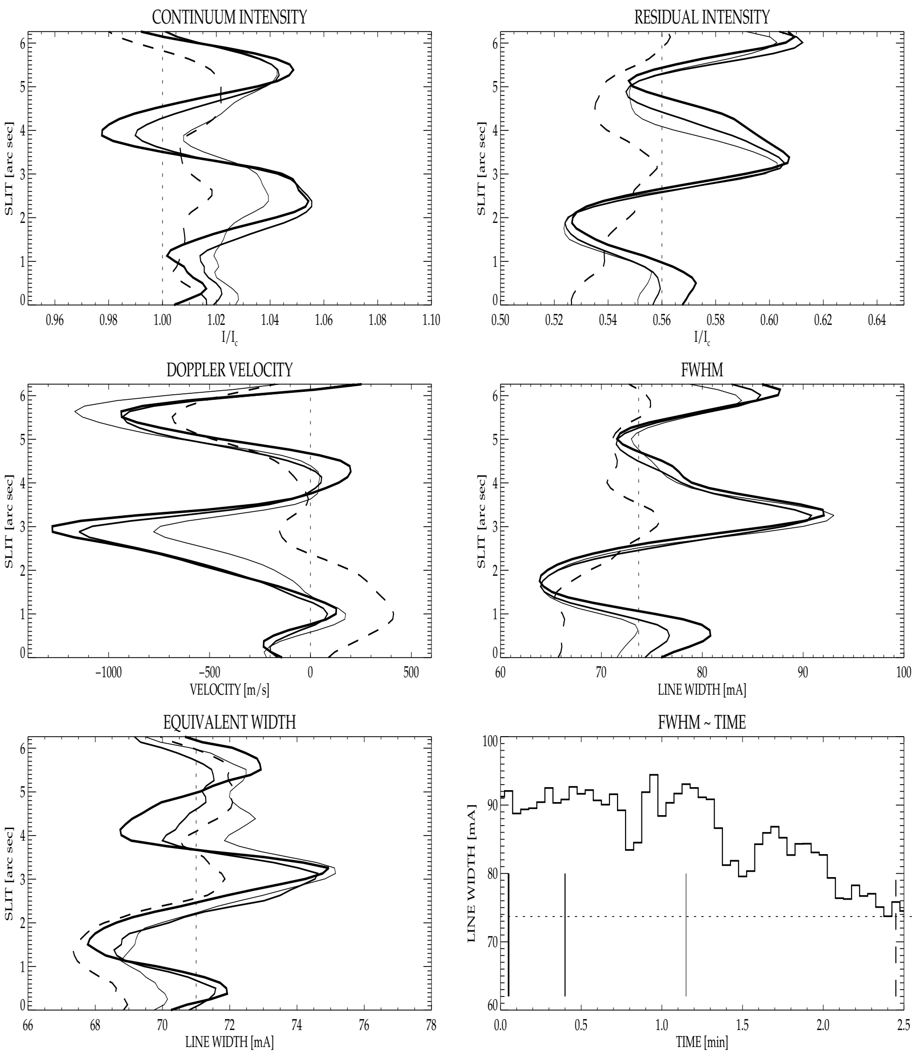

Figure 5: Spatial scans of the spectral characteristics for three moments of the shock event (solid lines of different thickness) and for the reference moment (dashed line). The temporal evolution of the *fw* is shown at the bottom right panel. The selected moments are depicted by vertical lines of the corresponding line thickness used in plots of this figure. The spatial scale should be multiplied by a factor of 1.661 to get the real solar surface distances because of limb-effect projection. Dotted vertical lines in panels show the average values of the particular spectral characteristic.

A small but clear increase of the equivalent line width *ew* just for 4% of its average value was found to be co-spatial with the enhancement of the *fw*.

6. Discussion and conclusion

The basic properties of the measured shock signature are in agreement with the predictions of the numerical simulations obtained for the shocks outside the magnetic field concentrations. Namely, most of the facts and relations between the spectral characteristics confirm that the observed event belonged to the shocks of *type-a* or *type-b*.

The event is located on the border of a granule. This is marked by the largest gradient of continuum intensity. The position of the event is definitely between the granulum area and the middle of the intergranular lane. The event is co-spatial with the significant increase of the residual line intensity. It confirms that the plasma inside the event was heated up at the border of the granule.

The largest gradient of the Doppler velocity was detected inside the event. The total difference of the Doppler velocity across the event was greater then 1200 m/s. The plasma moved toward the observer on the limb side of the event with the line-of-sight velocity of more than 1000 m/s. At the position of the event this motion has stopped. Moreover the analysis show that there is no coincidence between the intergranular lane position, the downward motion and the enhancement of the *fw* in the middle and upper photospheric layers. This fulfill the conclusion of Solanki et al. 1996 that observations made on the limb could exclude the increase of the *fw* caused by the downward motion in the intergranular lane.

All these properties of the shock are in agreement with the predictions of Steffen & Freytag, (1991), Steffen et al., (1994), Solanki et al., (1996), Steiner et al., (1998) and Gadun, (2000). The final conclusion whether the supersonic plasma granular flow and shock detected in our observation are caused either by the swaying motion of the flux tube or by the granular flow not related to the magnetic field cannot be definitely answered.

Nevertheless according the G-band data which reflect partly the magnetic situation in the area we beleve that the supersonic flow and the shock are caused by the swaying motion of the flux tube.

Acknowledgements

The VTT is operated by the Kiepenheuer-Institut für Sonnenphysik, Freiburg, at the Observatorio del Teide of the Instituto de Astrofisica de Canarias. We thank M. Sigwarth and T. Berkefeld for operation of the AO during our campaign. This work was supported by grant VEGA 2/3015/23 and by the Deutsche Forschungsgemeinschaft grant (DFG 436 SLK 113/7). A. H. acknowledges the support of the

Austrian Fond zu Förderung der Wissenschaftlichen Forschung (13308). Finally we acknowledge our late colleague A.S. Gadun who has initiated this project on the base of the results of his numerical simulations of solar granulation.

References

Allende Prieto, C. & Garciá López, R. J., 1998, A&A, 131, 431

Cattaneo, F., Hulburt, N.E. & Toorme, J., 1989, in Stellar and Solar Granulation, eds. R.J. Rutten & G. Severino, (Kluwer, Dordrecht), 415

Cattaneo, F., Hulburt, N.E. & Toorme, J., 1990, ApJ, 349, L63

Deinzer, W., Hensler, G., Schüssler, M. & Weisshaar, E., 1984, A&A, 139, 426

Gadun, A. S., 2000, private communication

Gadun, A. S., Solanki, S. K. & Johannesson, A., 1999, A&A, 350, 1018

Grossman-Doerth, U., Schüssler, M. & Solanki, S. K., 1988, A&A, 206, L37

Knölker, M., Schüssler, M. & Weisshaar, E., 1988, A&A, 194, 257

Kurucz, R. L., 1990, Trans. IAU, XXB, 168 (CD-ROM 23)

Malagoli, A., Cattaneo, F. & Brummell, N.H., 1990, ApJ, 361, L33

Moore, C. E., 1972, A Multiplet Table of Astrophysical Interest, NSRDS-NBS 40 (NBS, Washington)

Moore, C. E., Minnaert, M. G. J., & Houtgast, J. 1966, The Solar Spectrum 2935 Å to 8770 ÅNBS Monograph 61, (NBS, Washington)

Nesis, A., Bogdan, T. J., Cattaneo, F., Hanslmeier, A., Knölker, M. & Malagoli, A., 1992, ApJ, 399, L99

Nordlund, Å., 1984, in Small-Scale Dynamical Processes in Quiet Stellar Atmospheres, ed. S. L. Keil (Sunspot, NM, USA), 181

Schröter, E. H., Soltau, D. & Wiehr, E., 1985, Vistas in Astronomy, 28, 519

Solanki, S. K. & Stenflo, J. O., 1985. A&A, 148, 123

Solanki, S. K., Rüedi, I., Bianda, M. & Steffen, M., 1996, A&A, 308, 623

Steffen, M., Ludwig, H.-G. & Krüss, A., 1989, A&A, 213, 371

Steffen, M. & Freytag, B., 1991, Reviews of Modern Astronomy, 4, 43

Steffen, M., Freytag, B. & Holweger, H., 1994, in Solar Magnetic Fields, ed. M. Schüssler & W. Schmidt (Cambridge University Press, Cambridge), 298

Stein, R.F. & Nordlund, Å., 1989, ApJ, 342, L95

Steiner, O., Grossman-Doerth, U., Knölker, M. & Schüssler, M., 1998, ApJ, 495, 468

Wöhl, H., Kučera, A., Rybák, J. & Hanslmeier, A., 2002, A&A, 394, 1077